KINETIC FUNCTIONS IN MAGNETOHYDRODYNAMICS WITH RESISTIVITY AND HALL EFFECT*

Dedicated to Professor James Glimm on the occasion of his 75th birthday

Philippe G. LeFloch

Laboratoire Jacques-Louis Lions, Centre National de la Recherche Scientifique,
Université Pierre et Marie Curie (Paris 6), 4 Place Jussieu, 75258 Paris, France
E-mail: pgLeFloch@gmail.com

Siddhartha Mishra

Seminar for Applied Mathematics, D-Math, ETH, HG, Raemistrasse, Zürich-8092, Switzerland
E-mail: siddharm@cma.uio.no

Abstract We consider a nonlinear hyperbolic system of two conservation laws which arises in ideal magnetohydrodynamics and includes second-order terms accounting for magnetic resistivity and Hall effect. We show that the initial value problem for this model may lead to solutions exhibiting complex wave structures, including undercompressive nonclassical shock waves. We investigate numerically the subtle competition that takes place between the hyperbolic, diffusive, and dispersive parts of the system. Following Abeyratne, Knowles, LeFloch, and Truskinovsky, who studied similar questions arising in fluid and solid flows, we determine the associated kinetic function which characterizes the dynamics of undercompressive shocks driven by resistivity and Hall effect. To this end, we design a new class of "schemes with controled dissipation", following recent work by LeFloch and Mohammadian. It is now recognized that the equivalent equation associated with a scheme provides a guideline to design schemes that capture physically relevant, nonclassical shocks. We propose a new class of schemes based on high-order entropy conservative, finite differences for the hyperbolic flux, and high-order central differences for the resistivity and Hall terms. These schemes are tested for several regimes of (co-planar or not) initial data and parameter values, and allow us to analyze the properties of nonclassical shocks and establish the existence of monotone kinetic functions in magnetohydrodynamics.

Key words hyperbolic conservation law; magnetohydrodynamics; magnetic resistivity; Hall effect; undercompressive shock; kinetic function

2000 MR Subject Classification 35L65; 74S10; 65M12

1   Introduction

Many problems in the physical, biological and engineering sciences are modeled by nonlinear hyperbolic systems of conservation laws, augmented with second- or higher-order regularization terms. In one space dimension, these partial differential equations take the form

$$u_t + f(u)_x = 0, \tag{1.1}$$

where u is the vector-valued unknown and the flux $f = f(u)$ is a prescribed, smooth vector-valued map. The above equation has to be supplemented with suitable initial data. The system (1.1) is said to be strictly hyperbolic provided the eigenvalues of the flux Jacobian $\nabla_u f$ are real and distinct.

It is well known that solutions to (1.1) develop propagating discontinuities (shock waves, contact discontinuities) in finite time, even from smooth initial data; hence, solutions of (1.1) are considered in the weak sense. On the other hand, weak solutions are not uniquely determined by their initial data, in general, and suitable admissibility criteria need be imposed in order to recover uniqueness for the initial value problem. These admissibility criteria are termed as "entropy conditions".

One natural requirement is based on a convex entropy function $U = U(u)$ and entropy flux $F = F(u)$ which, by definition, must satisfy the compatibility condition $\nabla_u U \, \nabla_u f = \nabla_u F$. Such an entropy pair exists for most models of physical interest, and one then imposes that physically-meaningful weak solutions to (1.1) also satisfy the entropy inequality

$$U(u)_t + F(u)_x \leq 0 \tag{1.2}$$

in the distributional sense.

Another related strategy consists of imposing pointwise conditions at shocks. For systems with genuinely non-linear characteristic fields, the natural conditions are Lax entropy inequalities [21, 22] and, for more general systems, the Liu entropy condition [32]. These conditions imply, in particular, a restriction on the number of characteristics that impinge on a shock from both sides. Shocks with the correct number of characteristics impinging on them are termed as classical or Lax shocks.

Following LeFloch [24–26], we are interested here in the case that weak solutions are generated by adding high-order regularization terms in the right-hand side of (1.1).

Recall first that for scalar conservation laws, any function U is associated with an entropy flux F, and by imposing all such inequalities (1.2) one ensures the uniqueness of entropy solutions to the Cauchy problem. Most system admits however a single entropy pair and, hence, the weak solutions are solely constrained by one entropy inequality. Moreover, a single entropy inequality is not sufficient to ensure uniqueness, whenever the flux does not satisfy a convexity or genuine nonlinearity condition.

Recall also that shocks with either greater or lesser number of characteristics impinging on them are termed as nonclassical, and are referred to as being overcompressive or undercompressive, respectively.

Then, motivated by physical applications, let us for instance consider the class of entropy

solutions to (1.1) generated by diffusive-dispersive regularizations in the generic form:

$$u_t^\epsilon + f(u^\epsilon)_x = \epsilon \left(B(u^\epsilon)\, u_x^\epsilon\right)_x + \kappa\, \epsilon^2 \left(C(u^\epsilon)\, u_{xx}^\epsilon\right)_x, \tag{1.3}$$

for some constants $\epsilon > 0$ and $\kappa \in \mathbb{R}$ and some matrix-valued maps B, C. One typical requirement on the dissipation matrix B is that is is non-negative with respect to the scalar product induced by the entropy U, that is,

$$\nabla^2 U\, B \geq 0.$$

Under some further restriction on C (see [25]), one formally deduces that the entropy inequality (1.2) does hold in the limit $\epsilon \to 0$. It turns out however that (1.2) does not provide sufficient information on the effect of diffusive-dispersive small-scales, and does not lead to a well-posed problem for the system of conservation laws (1.1).

The nature of waves associated to a specific regularization such as (1.3) is conveniently exhibited by solving the Riemann problem associated with (1.1), corresponding to the piecewise constant initial data

$$u(x,0) = \begin{cases} u_l, & x < 0, \\ u_r, & x > 0, \end{cases} \tag{1.4}$$

for given constant states u_l, u_r. For instance, recall that the Riemann problem associated with a strictly hyperbolic system with genuinely non-linear (or linearly degenerate) characteristic fields can be uniquely solved by a combination of Lax shocks, contact discontinuities, and centered rarefaction waves.

An illustrative example for the presence of non-classical shocks is provided by the scalar conservation law, with a cubic flux function:

$$u_t + (u^3)_x = 0. \tag{1.5}$$

The above flux is non-convex and thus is neither genuinely non-linear nor linearly degenerate. Diffusive-dispersive regularizations [16, 19, 25] do lead to nonclassical shocks for (1.5). These shocks do not satisfy the classical Oleinik entropy inequalities for scalar conservation laws. Furthermore they arise as limits of the diffusive-dispersive regularization:

$$u_t^\epsilon + ((u^\epsilon)^3)_x = \epsilon u_{xx}^\epsilon + \kappa \epsilon^2 u_{xxx}^\epsilon. \tag{1.6}$$

On the other hand, taking $\kappa = 0$ in (1.6) results in a diffusive approximation, for which all limiting solutions are classical and satisfy the Oleinik entropy conditions.

In fact, nonclassical shocks do exist for solutions of many interesting problems, for instance in the dynamics of phase transitions in material science [1, 2, 23, 36, 37, 42, 43], in thin film flows [4, 5, 30, 31], and in flows in porous media [3, 20] among other applications. These shocks are the limits of models including second- or higher-order regularization terms and, hence, are physically relevant.

Nonclassical shocks satisfy a single entropy inequality of the form (1.2) but may not be unique and additional conditions need to be imposed in order to select a unique nonclassical shock solution. Such conditions are expressed in terms of kinetic relations, which relate the entropy dissipation at a shock in terms of the shock speed. These kinetic relations are often monotone functions and lead to uniqueness results of solutions containing nonclassical shocks.

In the absence of explicit formulas, numerical methods are heavily used in the study of conservation laws (1.1). Many standard methods [33] are based on the finite volume methodology and rely on discretizing the domain into cells and updating the cell averages of the unknown. The update is determined by constructing suitable Godunov-type numerical fluxes. These schemes are very successful in approximating classical shocks.

It is much more difficult to approximate nonclassical shocks. As an example, consider the cubic scalar conservation law (1.5). It is not difficult to check that a standard Godunov-type monotone scheme always approaches classical shocks (satisfying the Oleinik entropy conditions) to (1.5). Standard methods need to be adapted in order to approximate nonclassical shocks.

The numerical approximation of nonclassical shocks has been investigated in various works [8, 9, 16, 24, 27, 28] where schemes with controled dissipation are developed, as they are called in [26]. The recent paper by LeFloch and Mohammadian [28] provides a detailed review of the state of the art and demonstrate the key role played by the equivalent equation associated with the scheme under consideration. The main requirement for a scheme with controled dissipation is that the equivalent equation should be an approximate version of the diffusive-dispersive regularization (1.3), after the diffusion and dispersion terms in (1.3) be approximated directly by high-order finite differences (for instance). Note that this is a key difference from standard shock-capturing schemes, in which the diffusion and dispersion terms are implicit introduced and depend on the algebraic structure of the discretization of the hyperbolic flux. The equivalent equation is essential in introducing the small scale information needed for capturing nonclassical shocks. Another crucial role is played by the entropy conservative numerical flux developed in [27, 29, 38, 39]. The resulting schemes satisfy discrete versions of the entropy inequality (1.2) and were initially introduced by Tadmor [38], then extended to third-order by LeFloch et al. [17, 19] and, finally, investigated under more general circumstances [8, 9, 27, 39].

LeFloch and Mohammadian [28] demonstrated the significance of the equivalent equation for schemes that approximate nonclassical shocks. A key point of the study was to numerically determine kinetic functions associated with schemes. These approximations of the kinetic relation serve to quantify the ability of a scheme for computing nonclassical shocks. It is demonstrated in [28] that increasing the order of accuracy of the discretization led to a better approximation of the kinetic relation.

This general presentation leads us precisely to our main objective of the present paper, i.e., extending the above technique to a model of magnetohydrodynamics. We consider a nonstrictly hyperbolic system of two conservation laws (discussed extensively in Section 2) arising in ideal magnetohydrodynamics (MHD) when magnetic resistivity and Hall effect terms are included. First of all, we establish here that certain solutions of this model do contain nonclassical shocks. Following [28], we then design a class of high-order, entropy conservative, finite difference schemes for this model, and we apply them to study the properties of the associated nonclassical shocks. Different regimes are studied and reveal the presence of a regime, where nonclassical shocks are formed. Numerical kinetic functions are computed, and we establish that they support the theory developed in [18], which however assumed strict hyperbolicity. Our results further validate LeFloch and Mohammadian's strategy [28] and demonstrate that proper discretization of the equivalent equation can be combined with entropy conservative flux discretizations, leading to a robust and accurate dissipation-controled method for the approxi-

mation of nonclassical shocks;

This paper is organized as follows. The MHD model of interest is described in Section 2 and then, in Section 3, we introduce a class of high-order schemes, including up to 10-th order of accuracy. Our numerical results are presented in Section 4, and numerical kinetic relations are plotted. Finally, the conclusions of this paper are summarized in Section 5.

2 Magnetohydrodynamics Model with Rresistivity and Hall Terms

The equations of ideal magnetohydrodynamics (MHD) form a physically important example of a system of conservation laws that is not strictly hyperbolic (coinciding eigenvalues of the flux Jacobian) and in addition, is not genuinely non-linear nor linearly degenerate [35]. These equations model the evolution of plasmas and occur in astrophysics, solar physics, electrical and aerospace engineering. In one space dimension, the equations read

$$
\begin{aligned}
&\rho_t + (\rho u_1)_x = 0, \\
&(\rho u_1)_t + \left(\rho u_1^2 + p + \frac{B_2^2 + B_3^2 - B_1^2}{2}\right)_x = 0, \\
&(\rho u_2)_t + (\rho u_1 u_2 - B_1 B_2)_x = 0, \\
&(\rho u_3)_t + (\rho u_1 u_3 - B_1 B_3)_x = 0, \\
&(B_2)_t + (u_1 B_2 - u_2 B_1)_x = 0, \\
&(B_3)_t + (u_1 B_3 - u_3 B_1)_x = 0, \\
&E_t + \left(\left(E + p + \frac{|B|^2}{2}\right)u_1 - (u \cdot B) B_1\right)_x = 0,
\end{aligned}
\tag{2.1}
$$

where ρ is the density, $u = (u_1, u_2, u_3)$ and $B = (B_1, B_2, B_3)$ are the velocity and magnetic fields, respectively, p is the thermal pressure, and E is the total energy. For simplicity, we assume here that E is determined by the equation of state of ideal gases:

$$
E = \frac{p}{\gamma - 1} + \frac{1}{2}\rho |u|^2 + \frac{1}{2} B^2,
\tag{2.2}
$$

where γ is the gas constant. Note that the divergence constraint for MHD equations [6] in one space dimension implies that the normal magnetic field B_1 is a constant in both space and time and appears in (2.1) as a parameter.

Due to the lack of strict hyperbolicity and non-convex, the solutions of the Riemann problem for the ideal MHD equation exhibit very complex wave structures, including compound wave patterns and both undercompressive and overcompressive intermediate shocks. In turn, there is no uniqueness for solutions to the Riemann problem for ideal MHD equations. See [40] for further details.

So far, there has been no systematic study of the properties of nonclassical shocks for the ideal MHD equations. In particular, the existence of associated kinetic relations is yet to be investigated. The existence of kinetic relations might pave the way for obtaining unique solutions for the Riemann problem associated with the ideal MHD equations. The main reason for the lack of such results is the formidable difficulty in dealing with a complicated 7×7 system. Consequently, simpler models mimicking some of the difficulties present in the ideal MHD equations have been proposed and studied.

One sub-model for ideal magnetohydrodynamics is provided by the following 2×2 system ([13–15, 18]):

$$v_t + ((v^2 + w^2)v)_x = 0,$$
$$w_t + ((v^2 + w^2)w)_x = 0. \tag{2.3}$$

A systematic derivation of this system from the ideal MHD equations (2.1) is described in [34]. The vector (v, w) represents the transverse components of the magnetic field in the ideal MHD equations (2.1). The model also arises independently in studying the solar wind [10, 44] and in non-linear elasticity [7].

The system (2.3) is rotationally invariant,and smooth solutions of (2.3) can be parameterized in radial coordinates:

$$v = r\cos(\theta), \quad w = r\sin(\theta), \quad r \geq 0, \quad \theta \in [0, 2\pi), \tag{2.4}$$

so that (2.3) takes the form

$$r_t + 3r^2 r_x = 0,$$
$$\theta_t + r^2 \theta_x = 0. \tag{2.5}$$

The two eigenvalues of (2.3) are $\lambda_1 := r^2$ and $\lambda_2 := 3r^2$. Hence, the system is strictly hyperbolic except at the umbilic point $r = 0$. The characteristic field associated with $\lambda_2 = 3r^2$ is the fast mode of the system and fails to be genuinely non-linear. On the other hand, the slow or rotational mode is given by $\lambda_1 = r^2$. It is linearly degenerate as the mode is independent of θ.

The model (2.3) is neither strictly hyperbolic nor genuinely non-linear and mimics the structure of ideal MHD equation (2.1). There are two main wave families for (2.3) (cf. [13, 18]):

• Rotational discontinuities. These waves are associated with the slow (or rotational) mode; the radius r is constant and the angle θ varies across these waves.

• Fast waves. These waves keep the angle θ constant and are associated with the fast mode; the radius r varies across these waves.

One aim is to construct solutions to the Riemann problem associated with (2.3) in terms of the above wave families. However, this is not possible ([13, 18]) when the data are coplanar, i.e., when $w = cv$, for some constant c. In this case, (2.3) reduces formally to the following scalar conservation law with cubic flux:

$$v_t + (1 + c^2)(v^3)_x = 0. \tag{2.6}$$

As recalled in the introduction, solutions to (2.6) may contain nonclassical shocks. In the present paper, we go beyond the standard diffusive-dispersive regularization, and consider the following regularization of (2.3):

$$v_t^\epsilon + (((v^\epsilon)^2 + (w^\epsilon)^2)v^\epsilon)_x = \epsilon v_{xx}^\epsilon + \alpha\epsilon w_{xx}^\epsilon,$$
$$w_t^\epsilon + (((v^\epsilon)^2 + (w^\epsilon)^2)w^\epsilon)_x = \epsilon w_{xx}^\epsilon - \alpha\epsilon v_{xx}^\epsilon \tag{2.7}$$

for some positive constants ϵ, α. The diffusive term $\epsilon v_{xx}^\epsilon, \epsilon w_{xx}^\epsilon$ models magnetic resistivity while the dispersive ones $\alpha\epsilon v_{xx}^\epsilon, \alpha\epsilon w_{xx}^\epsilon$ models the Hall effect [44]. As observed by Hayes and LeFloch [18], nonclassical shocks to (2.3) do arise as limits of (2.7).

The system (2.3) admits an entropy function associated with the total energy

$$U(v, w) := \frac{1}{2}(v^2 + w^2), \quad F(v, w) = \frac{3}{4}((v^2 + w^2)^2). \tag{2.8}$$

which is compatible with the regularization (2.7). Weak solutions to (2.3) realized as limits of (2.7) then satisfy the entropy inequality

$$U(v, w)_t + F(v, w)_x \leq 0 \tag{2.9}$$

in the distributional sense. The properties of nonclassical shocks to (2.3) is summarized in the following theorem established in [18].

Theorem 2.1 Consider the Riemann problem for (2.3) with Riemann data (v_l, w_l) and (v_r, w_r). For non co-planar data, there exists a unique solution of the Riemann problem satisfying (2.9), which consists of a rotational discontinuity plus a fast shock or a rarefaction wave.

If the data are co-planar and the angles associated with initial data satisfy $\theta_r = \theta_l(\text{mod. } \pi)$, then the Riemann problem for (2.3) has a unique solution consisting of either a classical shock or a rarefaction wave.

If the data are co-planar and $\theta_r = \pi + \theta_l(\text{mod. } \pi)$, then the Riemann problem for (2.3) admits a one-parameter family of entropy solutions containing a nonclassical shock connecting (v_l, w_l) with an intermediate state (v_m, w_m), followed by a fast shock or a rarefaction. The nonclassical shocks are characterized uniquely via a kinetic relation of the form:

$$\varphi(s) = -s\frac{1}{2}[\![v^2 + w^2]\!] + \frac{3}{4}[\![(v^2 + w^2)^2]\!], \tag{2.10}$$

where $[\![a]\!]$ denotes the jump of a variable a and s denotes the shock speed, and φ satisfies the inequalities

$$\frac{\partial \varphi(s)}{\partial s} \geq 0, \qquad -\frac{3}{4} \leq \frac{\varphi(s)}{s^2} \leq 0. \tag{2.11}$$

The kinetic function (2.10) expresses the entropy dissipation as a monotone function of the shock speed. In [18], the authors also proved that the solutions of the diffusive-dispersive regularatization (2.7) converge to weak solutions to (2.3), by using the compensated compactness method. Thus, nonclassical shocks arise as limits of the diffusive-dispersive regularization (2.7), and our aim in this paper is to study numerically the property of nonclassical shocks, by using finite difference schemes well-adapted to the approximation of the system (2.3).

3   A Class of Difference Schemes with Controlled Dissipation

Preliminaries For simplicity, we consider a uniform discretization of the computational domain, with mesh size Δx and i-th mesh point $x_i := i\Delta x$. We discretize (2.7) directly, and more precisely

$$u_t + f(u)_x = D u_{xx}, \tag{3.1}$$

where $u := (v, w)$ and

$$f(u) := \Big((v^2 + w^2)v, (v^2 + w^2)w\Big), \qquad D = \begin{pmatrix} \epsilon(\Delta x) & \alpha\epsilon(\Delta x) \\ -\alpha\epsilon(\Delta x) & \epsilon(\Delta x) \end{pmatrix}.$$

The diffusion ϵ and the Hall coefficient $\alpha\epsilon$ depend explicitly on the mesh parameter Δx.

By denoting by $u_i(t)$ an approximation of $u(x_i, t)$ at time t, a conservative semi-discrete finite difference scheme for (3.1) takes the form (cf. for instance [33]):

$$\frac{\mathrm{d}}{\mathrm{d}t}u_i + \frac{1}{\Delta x}(f_{i+1/2}^d - f_{i-1/2}^d) = \frac{1}{\Delta x^2} R_i^d. \tag{3.2}$$

where $f_{i+1/2}^d$ is a discretization consistent with the exact hyperbolic flux and with spatial order of accuracy, and R_i^d denotes the discretization of the diffusion-dispersion terms. We have dropped the explicit t-dependence of all the quantities for notational convenience.

Standard finite difference flux   The first numerical flux we use is the standard centered finite difference flux:

$$f_{i+1/2}^{2p} = \sum_{j=1}^{p} \beta_j \overline{f}(u_i, u_{i+p}), \tag{3.3}$$

where $d = 2p$ is the order of the discretization and the flux $\overline{f}$ is given by the average:

$$\overline{f}(u_l, u_r) := \frac{1}{2}\big(f(u_l) + f(u_r)\big), \tag{3.4}$$

The coefficients β in (3.3) are determined from the requirement that the discretization is $2p$-th order accurate. The coefficients for discretizations up to 10-th order of accuracy are listed in Table 1. The resulting scheme may not satisfy a discrete version of the entropy inequality (2.9).

Table 1   Coefficients β in (3.3)

Order 2p	β_1	β_2	β_3	β_4	β_5
2	1				
4	$\dfrac{4}{3}$	$-\dfrac{1}{6}$			
6	$\dfrac{3}{2}$	$-\dfrac{3}{10}$	$\dfrac{1}{30}$		
8	$\dfrac{8}{5}$	$-\dfrac{2}{5}$	$\dfrac{8}{105}$	$-\dfrac{1}{140}$	
10	$\dfrac{5}{3}$	$-\dfrac{10}{21}$	$\dfrac{5}{42}$	$-\dfrac{5}{207}$	$\dfrac{1}{630}$

Entropy conservative flux discretization   Since the entropy inequality plays a role in the structure of the nonclassical shocks (see Theorem 2.1), it is more natural to rely on a scheme that satisfies a discrete entropy inequality. The starting point for designing an entropy stable scheme is the construction of an entropy conservative discretization of the flux f in (3.1). We use the terminology given by Tadmor [38] and the high-order schemes proposed by LeFloch et al. [27].

Consider (3.1) with the entropy function E and entropy flux Q given in (2.8) and define

$$S := \nabla_u U, \quad \psi := \langle S, f \rangle - F.$$

The vector S is called the entropy variable, while ψ is termed the entropy potential [38]. For the system (2.3), these quantities are explicitly calculated as

$$S = (v, w), \quad \psi = -\frac{1}{2}(v^2 + w^2)^2. \tag{3.5}$$

A $2p$-th order accurate entropy conservative numerical flux for (2.3) was proposed in [27]:

$$f_{i+1/2}^{2p} = \sum_{j=1}^{p} \beta_j \widetilde{f}(u_i, u_{i+p}), \tag{3.6}$$

with coefficients β listed in Table 1. The numerical flux $\widetilde{f}$ is any two point numerical flux function [38]:

$$\langle (S_r - S_l), \widetilde{f}(u_l, u_r) \rangle = \psi_r - \psi_l, \tag{3.7}$$

where u_l, u_r are any two states. For further results in the consistency and accuracy of the numerical fluxes (3.6), we refer to [39]. Finally, following [12], we deduce the following explicit formula for the entropy conservative flux:

$$
\begin{aligned}
\widetilde{f}(u_l, u_r) &= \left(\widetilde{f}_1(u_l, u_r), \widetilde{f}_2(u_l, u_r) \right), \\
\widetilde{f}_1(u_l, u_r) &:= \left(\frac{v_l^2 + v_r^2}{2} + \frac{w_l^2 + w_r^2}{2} \right) \frac{v_l + v_r}{2}, \\
\widetilde{f}_2(u_l, u_r) &:= \left(\frac{v_l^2 + v_r^2}{2} + \frac{w_l^2 + w_r^2}{2} \right) \frac{w_l + w_r}{2},
\end{aligned} \tag{3.8}
$$

which is clearly consistent with f in (3.1). Note that the entropy conservative flux is different from the centered flux (3.4).

Discretization of the diffusive-dispersive term   We use standard central finite differences of the appropriate order to discretize the diffusive-dispersive term in (3.2). Discretization of up to tenth-order of accuracy take the form:

• Second-order:
$$R_i^2 = u_{i+1} - 2u_i + u_{i-1}.$$

• Fourth-order:
$$R_i^4 = -\frac{1}{12}u_{i-2} + \frac{4}{3}u_{i-1} - \frac{5}{2}u_i + \frac{4}{3}u_{i+1} - \frac{1}{12}u_{i+2}.$$

• Sixth-order:
$$R_i^6 = \frac{1}{90}u_{i-3} - \frac{3}{20}u_{i-2} + \frac{3}{2}u_{i-1} + \frac{49}{18}u_i + \frac{3}{2}u_{i+1} - \frac{3}{20}u_{i+2} + \frac{1}{90}u_{i+3}.$$

• Eighth-order:
$$
\begin{aligned}
R_i^8 = &-\frac{1}{560}u_{i-4} + \frac{8}{315}u_{i-3} - \frac{1}{5}u_{i-2} + \frac{8}{5}u_{i-1} - \frac{205}{72}u_i \\
&+ \frac{8}{5}u_{i+1} - \frac{1}{5}u_{i+2} + \frac{8}{315}u_{i+3} - \frac{1}{560}u_{i+4}.
\end{aligned}
$$

• Tenth-order:
$$
\begin{aligned}
R_i^{10} = &\frac{1}{3150}u_{i-5} - \frac{5}{1008}u_{i-4} + \frac{5}{126}u_{i-3} - \frac{5}{21}u_{i-2} + \frac{5}{3}u_{i-1} - \frac{5269}{1800}u_i \\
&+ \frac{5}{3}u_{i+1} - \frac{5}{21}u_{i+2} + \frac{5}{216}u_{i+3} - \frac{5}{1008}u_{i+4} + \frac{1}{3150}u_{i+5}.
\end{aligned}
$$

Combining the entropy conservative fluxes (3.6), (3.8) with central discretizations of the diffusive-dispersive term is expected to ensure that the scheme (3.2) satisfies a discrete version of the entropy inequality (2.9); for details see [8, 9, 27, 29]. The time integration for the semi-discrete scheme (3.2) is performed by using a standard Runge-Kutta time stepping routine of the appropriate order.

4   Existence of Nonclassical Shocks and Kinetic Functions

Preliminaries   For the sake of reference, we denote the schemes introduced the previous section as follows:

• FDd. The scheme (3.2) with the average flux (3.4), the finite differences (3.3) and a finite difference discretization of the diffusive-dispersive term. All the differences are of order d.

• ECd. The same scheme as above but with the entropy conservative fluxes (3.8) replacing the averages (3.4).

In the following numerical experiments, we use $d = 2, 4, 6, 8, 10$ and all the schemes are integrated in time with a standard fourth-order Runge Kutta method. The time step is determined by a CFL condition and we use a CFL number of 0.45 for all simulations. Moreover, the three free parameters in (3.2) are the mesh size Δx, the diffusion coefficient ϵ, and the Hall coefficient α. We are going to test for various values of these parameters in the sequel.

Theorem 2.1 and various numerical experiments revealed the existence of the following three regimes.

Classical regime   Theorem 2.1 states that solutions of Riemann problems for (2.3) with non co-planar data contains only classical shock waves and rotational discontinuities. We test this proposition with the following numerical experiment.

Numerical Test 1   The MHD system (3.1) is considered with the initial data:

$$r(x,0) = \begin{cases} 2.0, & x < 0.25, \\ 1.2, & \text{otherwise,} \end{cases} \qquad \theta(x,0) = \begin{cases} \dfrac{\pi}{3}, & x < 0.25, \\ \dfrac{11\pi}{24}, & \text{otherwise.} \end{cases} \tag{4.1}$$

The computational domain is taken to be the interval $[0, 2]$, and the exact solution (see [18]) consists of a rotational discontinuity and a fast shock. All the schemes led to very similar results in this case, and we present results obtained with the $EC6$ scheme in Figure 1. The state v, the radius and angle are plotted, the mesh size is $\Delta x = 0.005$, and we treat two different values of the coefficients ϵ and α. In all the cases, the $EC6$ scheme approximates the solution quite well. The radius remains constant across the rotational discontinuity and the angle is constant across the shock, as expected.

Reducing the value of ϵ from $\epsilon = 2$ to $\epsilon = 0.5$ results in some oscillations. However, the waves are resolved more sharply in this case. Changing the value of the Hall coefficient from $\alpha = 0$ to $\alpha = 2$ did not alter the qualitative features of the solution. There were some dispersive oscillations around the shock wave in the regime of high dispersion.

Other numerical experiments in the classical regime of non co-planar data demonstrated very similar results.

Pseudo nonclassical regime   Theorem 2.1 indicates that the classical regime should consist of all states that are non co-planar. However, numerical experiments revealed an interesting "pseudo nonclassical" regime of initial states. By definition, in this regime, the difference in initial angle between the states is close to π. The resulting anomaly is illustrated in the following numerical experiment.

(a) $\epsilon = 2\Delta x$, $\alpha = 0$ (b) $\epsilon = 2\Delta x$, $\alpha = 2.0$

(c) $\epsilon = 5\Delta x$, $\alpha = 0$ (d) $\epsilon = 2\Delta x$, $\alpha = 2.0$
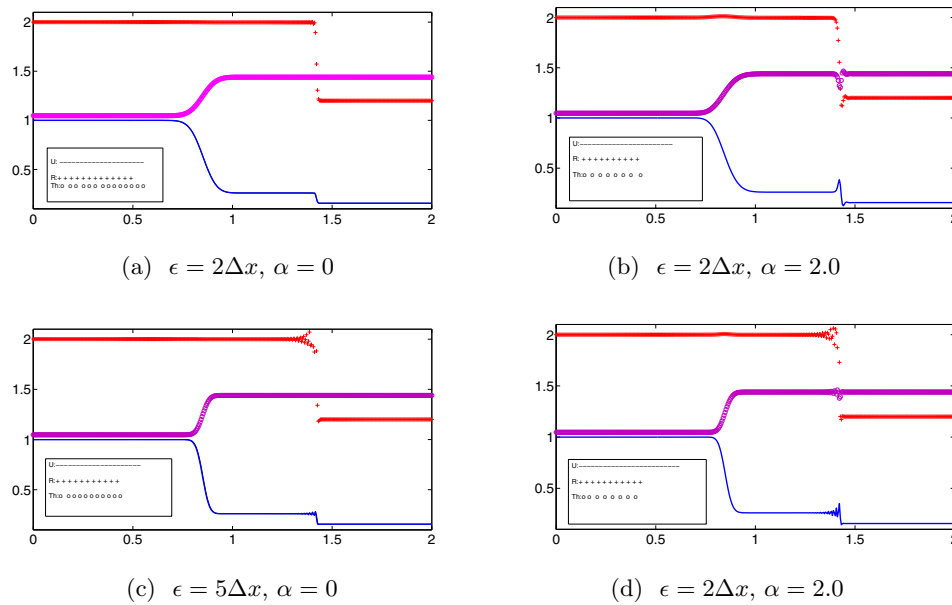
Fig.1 Test 1 with 400 mesh points at time $t = 1$. The plot shows the computed radius, angle, and variable v. Note that there are two waves in v but only one in the radius and the angle.

Numerical Test 2   We consider (2.3) with the initial data

$$r(x,0) = \begin{cases} 2.0, & x < 0.25, \\ 1.2, & \text{otherwise}, \end{cases} \qquad \theta(x,0) = \begin{cases} \dfrac{\pi}{3}, & x < 0.25, \\ \dfrac{29\pi}{24}, & \text{otherwise}. \end{cases} \tag{4.2}$$

Note that now $\theta_r - \theta_l = \frac{7\pi}{8}$ and the data is still non co-planar. However $\theta_r - \theta_l \approx \pi$. By Theorem 2.1, the exact solution consists of a rotational discontinuity and a fast shock. We tested with all the schemes and different sets of parameters, and again all the schemes led to very similar, but somewhat unexpected, results. For definiteness, in Figure 2. we present the plot for the scheme $EC6$.

We chose different sets of parameters. First, the mesh size is $\Delta x = 0.005$ (400 mesh points), the diffusion coefficient $\epsilon = 2\Delta x$ and the Hall coefficient α is set to zero. The results show that the radius is not constant across the rotational discontinuity. In fact, a middle wave is formed and the radius decreases across this wave. Characteristic analysis shows that this wave is an overcompressive nonclassical shock. This behavior apparently the conclusions of Theorem 2.1, but actually is a spurious numerical artifact.

The dispersive case ($\alpha = 2.0$) shows similar behavior. The middle wave is trailed by a overshoot, and reducing the diffusion coefficient to $\epsilon = 0.5\Delta x$ results in a much smaller middle wave. Increasing the mesh resolution by an order of magnitude (4000 mesh points) also results in reducing the amplitude of the middle wave. These two observations imply that the middle wave will disappear in the limit either by taking the mesh size to zero or by letting ϵ to go to zero. Hence, the middle wave is a entirely numerical.

The appearance of the middle wave leads to very slow convergence for the schemes. This is demonstrated in Figure 3 where we plot the results with the scheme $EC6$ for a mesh of 20000

points. The middle wave is still evident and there is a overshoot in the angle at the rotational discontinuity. Thus, the spurious nonclassical shock slows the convergence considerably. This phenomenon was also observed in [15] in a different context that did not take into account the Hall effect and relies on a particular finite volume scheme.

(a) $\epsilon = 2\Delta x$, $\alpha = 0$, 400 points   (b) $\epsilon = 2\Delta x$, $\alpha = 2.0$, 400 points

(c) $\epsilon = 0.5\Delta x$, $\alpha = 0$, 400 points   (d) $\epsilon = 2\Delta x$, $\alpha = 0$, 4000 points
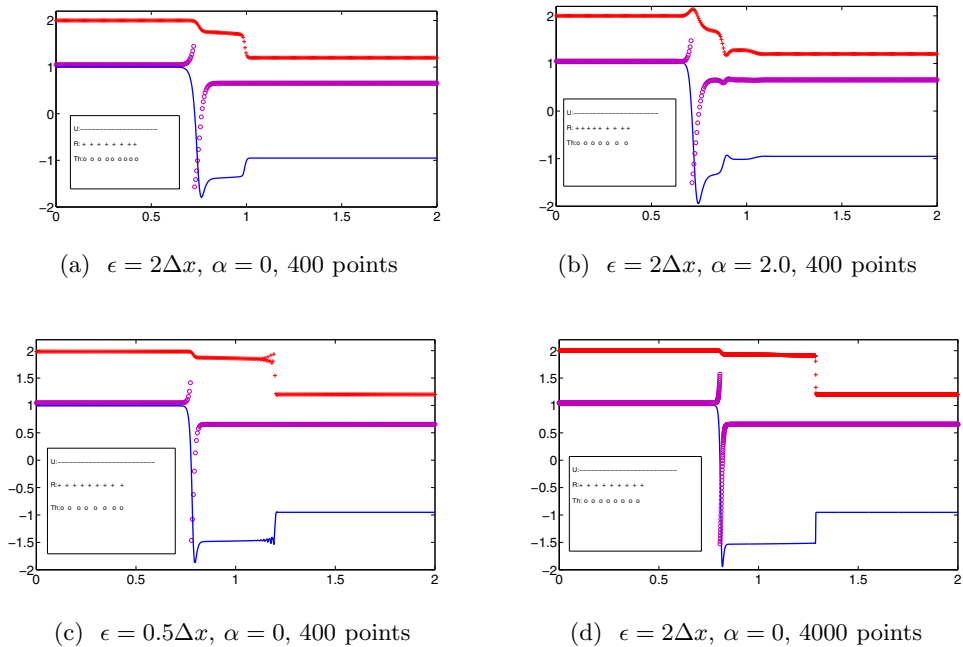
Fig.2   Test 2 at time $t = 1$. The plots show the radius, angle and the unknown v. Note the spurious middle wave characterized by a jump in the radius and the angle.
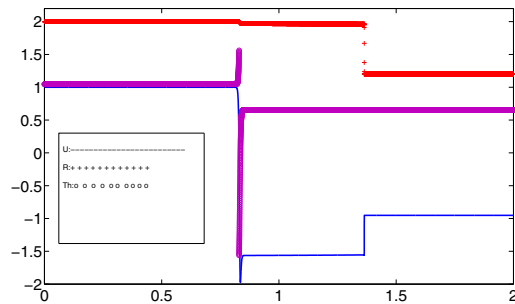
Fig.3   Test 2 with 20000 points. The radius, angle and v are plotted.

Our results show that this behavior is independent of the approximation scheme. Furthermore, it persists even in the presence of dispersion generated by the Hall terms. Interestingly enough, a similar pseudo-convergence was also pointed out by Torilhon in computations with the full MHD equations [40, 41]. We note that the simplified model studied in the present paper allows us to more clearly identify this phenomena.

Nonclassical regime   The most interesting behavior is observed with coplanar initial

data. Indeed, Theorem 2.1 suggests that the solutions to (2.3) contain nonclassical shock waves when the data are co-planar and the difference in the initial angles is π. We have investigated this regime extensively and aimed at plotting numerical kinetic relations, for the schemes introduced in this paper. Let us consider the Riemann data

$$r(x,0) = \begin{cases} r_l, & x < 0.25, \\ 0.6r_l, & \text{otherwise,} \end{cases} \qquad \theta(x,0) = \begin{cases} 0, & x < 0.25, \\ \pi, & \text{otherwise,} \end{cases} \tag{4.3}$$

where r_l is regarded as a free parameter and, by construction, the difference between the two initial angles is π.

Numerical Test 3   Consider (3.1) with the initial data (4.3) and the parameter value $r_l = 4$. We compute with all the entropy conservative schemes (3.6) and show the computed radius in Figure 4.

(a) $\epsilon = \Delta x,\, \alpha = 0$ (b) $\epsilon = \Delta x,\, \alpha = 2.0$
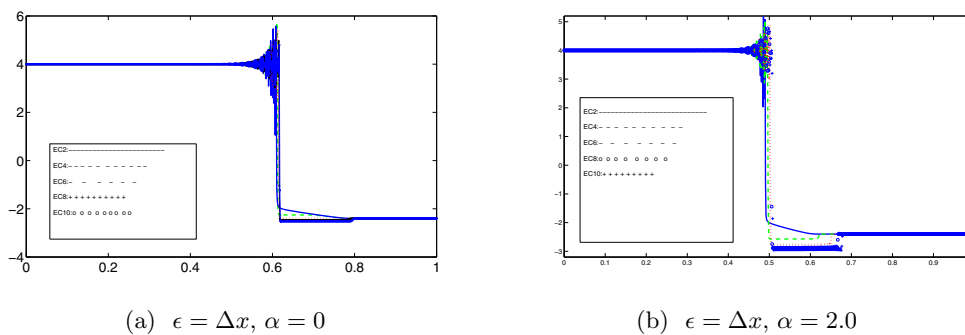
Fig.4   Radius r for Test 3 at time $t = 0.1$ and 800 mesh points.

The parameters are taken to be $\epsilon = \Delta x$ and two different Hall coefficents are tested, i.e., $\alpha = 0.0$ and $\alpha = 2.0$. Since the initial jump is large, one expects oscillations behind the shocks. Figure 4 shows that the second-order $EC2$ scheme computes a classical solution consisting of a classical shock followed by a rarefaction wave. However, the higher-order schemes approximate a solution consisting of a nonclassical shock and a fast shock. Note that the approximation improves if we increase the order of the scheme. This is quantified by observing the intermediate state and the shock speed. Furthermore, there is little qualitative difference between the purely diffusive case ($\alpha = 0$) and the large dispersion case ($\alpha = 2$). The large dispersion leads to even smaller values of the intermediate state and hence larger speeds for the nonclassical shock. There is a marked difference between the classical and the nonclassical regimes, and comparing Figures 1 and 4 illustrates that difference quite clearly.

Comparison between centered finite differences (3.3) and entropy conservative fluxes (3.6)   There are minor differences between the standard FD and the entropy conservative EC schemes in either the classical regime or the pseudo nonclassical regime. However, there are some noticeable differences between these two schemes in the nonclassical regime. This difference is apparent when initial data with large jumps are considered and strong nonclassical shocks are generated, as we now show.

Numerical Test 4   Now, we take $r_l = 8$ in (4.3), and the coefficients are $\epsilon = \Delta x$ and

$\alpha = 0$. We compute with the schemes $FD6$ and $EC6$, on a mesh with 4000 mesh points, until the time $t = 0.05$, and we plot the computed radius in Figure 5.

Hence, both schemes approximate a nonclassical shock and a fast shock. The main differences lie in the fact that the results with the $EC6$ scheme exhibit a larger intermediate state. High frequency oscillations are clearly observed with the scheme $FD6$, around the intermediate state. This makes it very difficult to ascertain the exact value of the intermediate state computed by the $FD6$ scheme.
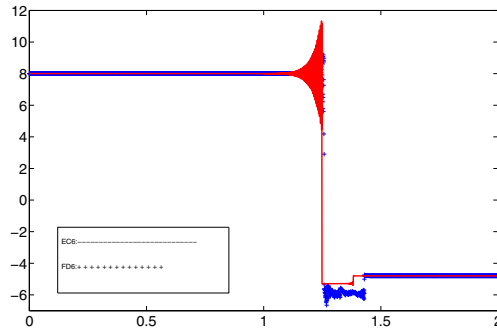
Fig.5   Radius with the $EC6$ and $FD6$ schemes for Test 4 with $\epsilon = \Delta x$, $\alpha = 0$ and 4000 mesh points.

Numerical kinetic functions   We arrive at the main contribution of the present paper and compute numerical kinetic relations that characterize the dynamics of nonclassical shocks in (2.3). As observed in [16, 28], the task of computing numerical kinetic relations is quite delicate. A large number of numerical experiments need to be performed and a large set of parameter values have to be considered.

We consider different initial data in the nonclassical regime and compute the intermediate state numerically. This allows us to compute the shock speed and the entropy dissipation (2.10) across the nonclassical shock. For very weak nonclassical shocks, the intermediate state lies close to the initial states and it is difficult to determine it exactly. When the nonclassical shock is strong, there are high frequency and large amplitude oscillations around the shocks. These oscillations (see Figure 5) obscure the intermediate state. Hence, it is almost impossible to obtain kinetic relations with the FD schemes, at least for strong nonclassical shocks. We will compute numerical kinetic relations with the EC schemes.

The diffusion coefficient is fixed as $\epsilon = \Delta x$ for all simulations. There were very minor differences in results when other values of the diffusion coefficient were considered. The parameter r_l in (4.3) takes all positive integers up to 20 as values. For a fixed r_l, we experimented with different mesh sizes and selected a mesh size with sufficient resolution. The intermediate state was calculated and used to compute the shock speed and the entropy dissipation across the nonclassical shock. We plot the intermediate state as a function of the initial r_l in the left-hand column of Figure 6. This is an indicator for the nonclassical behavior of the solutions ([28]). The right-hand column of Figure 6 shows the kinetic relation, more precisely, the scaled entropy dissipation (2.10) (or driving force) as a function of the shock speed.

Three different values of the Hall coefficient α were used. For the pure diffusion case

($\alpha = 0$), the results are shown in the top row of Figure 6. They demonstrate that the second-order $EC2$ scheme approximates a classical solution for all values of r_l. The classical solution is a compound shock (see Figure 4) and the corresponding kinetic relation is trivial. On the other hand, the high-order schemes approximate the nonclassical shock. The quality of approximation improves with the order of the scheme. The kinetic relation is approximately monotone, even for very strong shocks and very high shock speeds. In contrast to the results of [28], we are able to obtain monotonicity of the numerical kinetic relations even for very strong shocks. A possible reason might lie in the use of entropy conservative schemes.

(a) $\epsilon = \Delta x$, $\alpha = 0$

(b) $\epsilon = \Delta x$, $\alpha = 0$

(c) $\epsilon = \Delta x$, $\alpha = 1$

(d) $\epsilon = \Delta x$, $\alpha = 1$

(e) $\epsilon = \Delta x$, $\alpha = 2$

(f) $\epsilon = \Delta x$, $\alpha = 2$
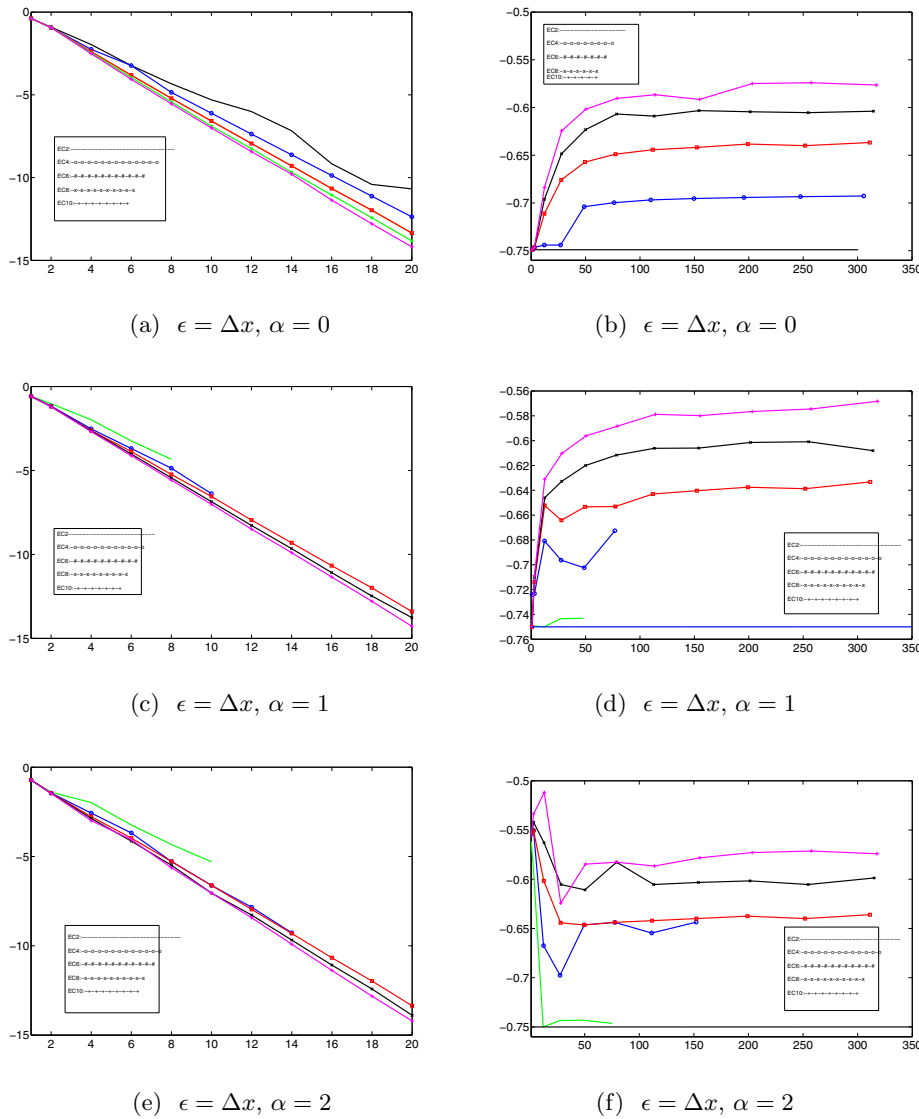
Fig.6 Numerical kinetic relations for the EC schemes. Left column: Intermediate radius (vertical axis) versus left-hand radius r_l (horizontal axis), Right column: Scaled entropy dissipation ($\frac{\varphi(s)}{s^2}$, (2.10)) (vertical axis) versus shock speed s (horizontal axis). Top row: $\alpha = 0$, Middle row: $\alpha = 1$, Bottom Row: $\alpha = 2$.

A moderate amount of dispersion, corresponding to $\alpha = 1.0$ leads to some differences from the pure diffusion case. Even the low-order $EC2$ approximates a nonclassical shock in this case. However, the nonclassical shock approximated by the $EC2$ scheme exhibit very high-frequency oscillations. These oscillations increase considerably when stronger shocks are considered. The $EC2$ scheme can no longer be used to compute the kinetic relation when this happens. This breakdown is represented with a broken curve, and similar behavior is noticed for the $EC4$ scheme. On the other hand, the even higher order $EC6, EC8$ and $EC10$ schemes approximate the nonclassical shock quite well. The numerical kinetic relation continues to be monotone, even for very large shock speeds.

Increasing the dispersion and considering now $\alpha = 2$, we are led to an equally interesting outcome. The low-order $EC2$ and $EC4$ schemes approximate the nonclassical shock initially, but break down due to large oscillations when the shock strength is increased. Also, an "initial" layer appears in the numerical kinetic functions for the high-order EC schemes. The kinetic function is initially oscillatory but recovers monotonicity when the shock speed is increased. The oscillations in the kinetic relation for small shocks might just have to do with the failure to obtain the correct values of the intermediate state for very weak shocks. Dispersion influences the quality of numerical kinetic relations considerably.

In the absence of explicit formulas for calculating the intermediate state or the entropy dissipation, it is difficult to establish the convergence of the numerical kinetic functions shown in Figure 6 as the order of the schemes is increased. The evidence presented in the figure does not appear to be conclusive. Consequently, we would like to investigate the experimental convergence of the numerical kinetic functions.
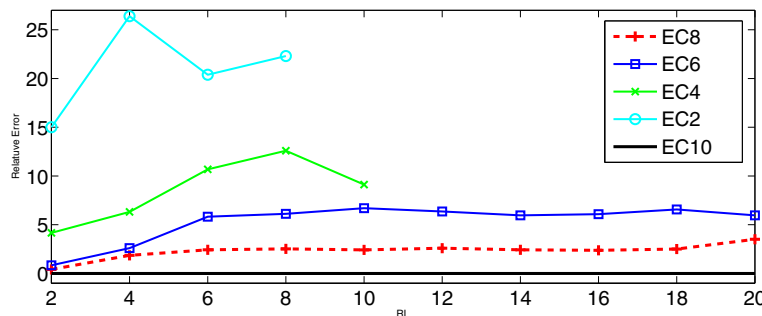
Fig.7   Relative error (4.4) (vertical axis) versus r_l (horizontal axis) with the EC schemes for $\alpha = 1$.

Let r_l denote the left-hand value of the radius in the Riemann problem (4.3) and $r_l^m(d)$ denote the intermediate radius computed with the ECd scheme. In the absence of formulas for computing the exact intermediate state, we assume that $r_l^m(10)$ is a good approximation for the exact intermediate state and employ it as a reference solution. We denote

$$\mathcal{RE}_d(r_l) = 100 \, \frac{|r_l^m(d) - r_l^m(10)|}{|r_l^m(10)|}, \tag{4.4}$$

as the relative error in the intermediate state for any given r_l. The aim is to examine whether

$\mathcal{RE}_d$ decreases as d is increased and at what rate. The relative errors for each r_l are computed for $\alpha = 1.0$ (moderate diffusion) and plotted against r_l in Figure 7. Note the experimental convergence as the order is increased. The results show that the $EC8$ scheme provides the best approximation to the reference solution with the $EC6$ scheme leading to consistently greater errors than the $EC8$ scheme. The $EC2$ and $EC4$ schemes are shown with broken curves as these schemes cannot be used for very strong shocks on account of heavy oscillations. When these schemes are stable, the $EC4$ scheme leads to greater errors than the $EC6$ scheme whereas the $EC2$ scheme leads to very large relative errors. The figure clearly indicates that the schemes are converging to the reference intermediate state as the order is increased. Furthermore, the convergence depends on the shock strength although there is a large region of the phase space where the rate of convergence appears to be independent of the shock strength. Similar convergence holds for the kinetic function as well as for different values of the dispersion parameter α.

5 Concluding Remarks

The ideal MHD equations (2.1) are non strictly hyperbolic, and admit characteristic fields that are neither genuinely non-linear nor linearly degenerate. Solutions to the MHD equations may contain undercompressive nonclassical shocks, which depend upon regularization and are obtained here as limits of a second-order diffusive-dispersive regularizations (2.7). The simplified system (2.3) analyzed in the present paper is rotational invariant and models the effect of the solar wind (as well as problems from non-linear elasticity). More precisely, solutions to this system exhibit nonclassical shocks for co-planar initial data, and uniqueness of these solutions is ensured only by imposing an additional admissibility criteria, i.e., a kinetic relation.

In this paper, we have investigated the wave structure of solutions to (2.3) numerically. The equation (3.1) including small scale effects (resistivity, Hall effect) was discretized by a class of high-order finite difference schemes. In particular, we have designed a novel class of schemes based on entropy conservative flux discretizations and an analysis of the equivalent equation. The second-order diffusive-dispersive terms were discretized by high-order central finite differences.

The resulting schemes were tested on a wide variety of numerical experiments, and our results allow us to distinguish between three distinct regimes. In the classical regime, only classical shocks are observed. In a pseudo nonclassical regime, the initial data are very close to co-planar data, and we observe that spurious nonclassical shocks are formed. Interestingly enough, these shocks are eliminated by reducing the mesh size (or the magnitude of the regularization coefficient) and the solution converges to the classical solution in the limit. However, this convergence is very slow. These observations are consistent with the results of [15, 41] which did not include the (dispersive) Hall effect.

Last but not least, the most interesting regime is when the data are precisely co-planar, and the solutions do include nonclassical shocks. We have determined numerically kinetic relations for different choices of dispersion coefficients. We observed that standard finite difference schemes led to unacceptably large oscillations for strong shocks. High-order accurate, entropy conservative schemes [27, 29, 38, 39] were found to provide good accuracy for the kinetic re-

lations. On the other hand, lower order schemes are found to lead to non-monotone kinetic relations and break down at strong shocks. The role of the dispersion associated with the Hall effect was also discussed in detail.

Our results provide further support to the use of schemes with controled dissipation advocated in the series of papers [8, 9, 16, 24, 26–29] and based on combining an analysis of the equivalent equations and entropy conservative flux discretizations. Indeed, our results suggest that the proposed toolkit of equivalent equations, entropy conservative schemes, and numerical kinetic relations should extend to the study of the full ideal MHD system (2.1).

References

[1] Abeyratne R, Knowles J K. Kinetic relations and the propagation of phase boundaries in solids. Arch Rational Mech Anal, 1991, **114**: 119–154

[2] Abeyratne R, Knowles J K. Implications of viscosity and strain-gradient effects for the kinetics of propagating phase boundaries in solids. SIAM J Appl Math, 1991, **51**: 1205–1221

[3] Avezedo A, Marchesin D, Plohr B J, Zumbrun K. Non-uniqueness of solutions of Riemann problems caused by 2-cycles of shock waves//Proc of Fifth International Conf on Hyperbolic Equations. Singapore: World Scientific, 1996: 43–51

[4] Bertozzi A, Münch A, Shearer M. Undercompressive shocks in thin film flows. Phys D, 1999, **134**: 431–464

[5] Bertozzi A, Shearer M. Existence of undercompressive traveling waves in thin film equations. SIAM J Math Anal, 2000, **32**: 194–213

[6] Biskamp D. Nonlinear magnetohydrodynamics, Cambridge monographs on plasma physics. Cambridge Univ Press, 1993

[7] Brio M, Hunter J. Rotationally invariant hyperbolic waves. Comm Pure Appl Math, 1990, **43**: 1037–1053

[8] Chalons C, LeFloch P G. A fully discrete scheme for diffusive-dispersive conservation laws. Numerische Math, 2001, **89**: 493–509

[9] Chalons C, LeFloch P G. High-order entropy conservative schemes and kinetic relations for van der Waals fluids. J Comput Phys, 2001, **167**: 1–23

[10] Cohen R H, Kulsrud R M. Non-linear evolution of quasi-parallel propagating hydro-magnetic waves. Phys Fluid, 1974, **17**: 2215–2225

[11] Fan H T, Slemrod M. The Riemann problem for systems of conservation laws of mixed type//Shock Induced Transitions and Phase Structures in General Media. IMA Vol Math Appl 52. New York: Springer-Verlag, 1993: 61–91

[12] Fjordholm U S, Mishra S, Tadmor E. Energy preserving and energy stable schemes for the shallow water equations//Cucker F, Pinkus A, Todd M, eds. Foundations of Computational Mathematics, Hong Kong 2008. London Math Soc Lecture Notes Ser 363. London Math Soc, 2009: 93–139

[13] Freistühler H. Dynamical stability and vanishing viscosity: a case study of a non-strictly hyperbolic system of conservation laws. Comm Pure Appl Math, 1992, **45**: 561–582

[14] Freistühler H. Stability of nonclassical shock waves//Proc of Fifth International Conference on Hyperbolic Equations. Singapore: World Scientific, 1996: 120–129

[15] Freistühler H, Pitman E B. A numerical study of a rotationally degenerate hyperbolic system, Part 1: The Riemann problem. J Comput Phys, 1992, **100**: 306–321

[16] Hayes B T, LeFloch P G. Nonclassical shocks and kinetic relations: Scalar conservation laws. Arch Rational Mech Anal, 1997, **139**: 1–56

[17] Hayes B T, LeFloch P G. Nonclassical shocks and kinetic relations: Finite difference schemes. SIAM J Num Anal, 1998, **35**: 2169–2194

[18] Hayes B T, LeFloch P G. Nonclassical shocks and kinetic relations: Strictly hyperbolic systems. SIAM J Math Anal, 2000, **31**: 941–991

[19] Jacobs D, McKinney W R, Shearer M. Traveling wave solutions of a modified Korteweg De-Vries equation. J Diff Eqns, 1995, **116**: 448–467

[20] Keyfitz B, Kranzer H. A system of nonstrictly hyperbolic conservation laws arising in elasticity theory. Arch Rational Mech Anal, 1980, **72**: 219–241

[21] Lax P D. Hyperbolic systems of conservation laws, II. Comm Pure Appl Math, 1957, **10**: 537–566

[22] Lax P D. Hyperbolic systems of conservation laws and the mathematical theory of shock waves//Regional Confer Series in Appl Math 11. Philadelphia: SIAM, 1973

[23] LeFloch P G. Propagating phase boundaries: formulation of the problem and existence via the Glimm scheme. Arch Rational Mech Anal, 1993, **123**: 153–197

[24] LeFloch P G. An introduction to nonclassical shocks of systems of conservation laws//International School on Hyperbolic Problems, Freiburg, Germany, Oct 97. Kröner D, Ohlberger M, Rohde C, eds. Lect Notes Comput Eng, Vol 5. Springer-Verlag, 1999: 28–72

[25] LeFloch P G. Hyperbolic Systems of Conservation Laws: The Theory of Classical and Nonclassical Shock Waves. Lectures in Mathematics, ETH Zürich. Birkhäuser, 2002

[26] LeFloch P G. Kinetic relations for undercompressive shock waves. Physical, mathematical, and numerical issues. Centre for Advanced Study of the Norwegian Academy of Science and Letters. Holden H, Karlsen K, ed. 2010

[27] LeFloch P G, Mercier J M, Rohde C. Fully discrete entropy conservative schemes of arbitrary order. SIAM J Numer Anal, 2002, **40**: 1968–1992

[28] LeFloch P G, Mohammadian M. Why many theories of shock waves are necessary. Kinetic functions, equivalent equations and fourth-order models. J Comput Phys, 2008, **27**: 4162–4189

[29] LeFloch P G, Rohde C. High order schemes, entropy inequalities and nonclassical shocks. SIAM J Numer Anal, 2000, **37**: 2023–2060

[30] LeFloch P G, Shearer M. Nonclassical Riemann solvers with nucleation. Proc Royal Soc Edinburgh, 2004, **134A**: 941–964

[31] Levy R, Shearer M. Comparison of two dynamic contact line models for driven thin liquid films. European J Appl Math, 2004, **15**: 625–642

[32] Liu T P. The Riemann problem for general 2×2 conservation laws. Trans Amer Math Soc, 1974, **199**: 89–112

[33] LeVeque R J. Finite Volume Methods for Hyperbolic Problems. Cambridge: Cambridge Univ Press, 2002

[34] Myong R S, Roe P L. Shock waves and rarefaction waves in magnetohydrodynamics, Part 1. A model system. J Plasma Phys, 1997, **58**: 485–519

[35] Roe P L, Balsara D S. Note on the eigensystem of magnetohydrodynamics. SIAM J Appl Math, 1996, **56**: 57–67

[36] Slemrod M. Admissibility criteria for propagating phase boundaries in a van der Waals fluid. Arch Rational Mech Anal, 1983, **81**: 301–315

[37] Slemrod M. A limiting viscosity approach to the Riemann problem for materials exhibiting change of phase. Arch Rational Mech Anal, 1989, **105**: 327–365

[38] Tadmor E. The numerical viscosity of entropy stable schemes for systems of conservation laws, I. Math Comp, 1987, **49**: 91–103

[39] Tadmor E. Entropy stability theory for difference approximations of nonlinear conservation laws and related time-dependent problems. Acta Numerica, 2003, **12**: 451–512

[40] Torrilhon M. Uniqueness conditions for Riemann problems of ideal magneto-hydrodynamics. J Plasma Phys, 2003, **69**: 253–276

[41] Torrilhon M. Non-uniform convergence of finite volume schemes for Riemann problems of ideal magneto-hydrodynamics. J Comput Phys, 2003, **192**: 73–94

[42] Truskinovsky J. Dynamics of non-equilibrium phase boundaries in a heat conducting nonlinear elastic medium. J Appl Math and Mech (PMM), 1987, **51**: 777–784

[43] Truskinovsky L. Kinks versus shocks//Fosdick R, Dunn E, Slemrod M, ed. Shock Induced Transitions and Phase Structures in General Media. IMA Vol Math Appl, 52. New York: Springer-Verlag, 1993: 185–229

[44] Wu C C, Kennel C F. The small amplitude magnetohydrodynamic Riemann problem. Phys Fluids B, 1993, **5**: 2877–2886